



HAL
open science

2D multislice MP2RAGE sequence for fast T 1 mapping at 7 T: Application to mouse imaging and MR thermometry

Thibaut ; Faller, Aurélien Trotier, Alice Rousseau, Jean-michel Franconi, Sylvain Miraux, Emeline Ribot

► To cite this version:

Thibaut ; Faller, Aurélien Trotier, Alice Rousseau, Jean-michel Franconi, Sylvain Miraux, et al.. 2D multislice MP2RAGE sequence for fast T 1 mapping at 7 T: Application to mouse imaging and MR thermometry. *Magnetic Resonance in Medicine*, 2020, 84 (3), pp.1430-1440. 10.1002/mrm.28220 . hal-03033863

HAL Id: hal-03033863

<https://hal.science/hal-03033863>

Submitted on 8 Dec 2020

HAL is a multi-disciplinary open access archive for the deposit and dissemination of scientific research documents, whether they are published or not. The documents may come from teaching and research institutions in France or abroad, or from public or private research centers.

L'archive ouverte pluridisciplinaire **HAL**, est destinée au dépôt et à la diffusion de documents scientifiques de niveau recherche, publiés ou non, émanant des établissements d'enseignement et de recherche français ou étrangers, des laboratoires publics ou privés.



Development of a 2D Multi-Slice MP2RAGE sequence for fast T1 mapping at 7T: Application to mouse imaging and MR thermometry.

Journal:	<i>Magnetic Resonance in Medicine</i>
Manuscript ID	MRM-19-20322.R2
Wiley - Manuscript type:	Full Paper
Date Submitted by the Author:	n/a
Complete List of Authors:	Faller, Thibaut; Centre de résonance magnétique des systèmes biologiques, CNRS / Université de Bordeaux Trotier, Aurélien; Centre de résonance magnétique des systèmes biologiques, CNRS / Université de Bordeaux Rousseau, Alice; Centre de résonance magnétique des systèmes biologiques, CNRS / Université de Bordeaux Franconi, Jean-Michel; Centre de résonance magnétique des systèmes biologiques, CNRS / Université de Bordeaux Miraux, Sylvain; Centre de résonance magnétique des systèmes biologiques, CNRS / Université de Bordeaux Ribot, Emeline; Centre de résonance magnétique des systèmes biologiques, CNRS / Université de Bordeaux
Research Type:	Technical Research
Research Focus:	No specific tissue or organ focus

SCHOLARONE™
Manuscripts

1
2
3 **2D Multi-Slice MP2RAGE sequence for fast T1 mapping at 7T:**
4
5
6 **Application to mouse imaging and MR thermometry.**
7
8
9

10
11
12
13
14
15 Thibaut L Faller, MS,¹ Aurélien J trotier, PhD,¹ Alice F Rousseau, MS,¹ Jean-Michel

16
17 Franconi, PhD,¹ Sylvain Miraux, PhD,¹ and Emeline J Ribot, PhD¹

18
19
20 ¹Centre de Résonance Magnétique des Systèmes Biologiques, UMR 5536,

21
22 CNRS/Université de Bordeaux, 146 rue Léo Saignat, 33076 Bordeaux, France
23
24
25

26
27 **Corresponding author:** Emeline J Ribot

28
29 Centre de Résonance Magnétique des Systèmes Biologiques,

30
31 UMR 5536 CNRS/Université de Bordeaux

32
33 146 rue Léo Saignat, 33076 Bordeaux

34
35 Telephone / Fax: +33 5 57 57 10 20 / +33 5 57 57 45 56

36
37 Email: ribot@rmsb.u-bordeaux.fr
38
39
40
41
42
43

44 **Word count:** 4601

45
46 **Key words :** MP2RAGE, 2D Multi-slice, T1 mapping, mouse, Thermometry, 7T
47
48
49
50
51
52
53
54
55
56
57
58
59
60

Abstract

Purpose: To develop a 2D radial multi-slice (MS) Magnetization Prepared 2 Rapid Gradient Echoes (MP2RAGE) sequence for fast and reliable T_1 mapping at 7T in mice and for MR thermometry.

Methods: The 2D MP2RAGE sequence was performed with the following parameters: TI_1 - TI_2 -MP2RAGE_{TR} = 1000-3000-9000 ms. The multiple dead times within the sequence were used for interleaved multi-slice acquisition, enabling to acquire 6 slices in 9 s.

The excitation pulse shape, inversion selectivity and inter-slice gap were optimized. In vitro comparison with the Inversion Recovery sequence was performed. T_1 variations with temperature were measured on tubes with T_1 ranging from 800 to 2000 ms.

The sequence was used to acquire T_1 maps continuously during 30 minutes on the brain and abdomen of healthy mice.

Results: A three lobes cardinal sine excitation pulse, combined with an inversion slice thickness and an inter-slice gap of respectively 150 and 50 % of the imaging slice thickness led to a standard deviation and bias of the T_1 measurements below 1 and 2 %, respectively. A linear dependence of T_1 with temperature was measured between 10 and 60°C. In vivo, less than 1% variation was measured between successive T_1 maps in the mouse brain. In the abdomen, no obvious in-plane motion artifacts were observed but respiratory motion in the slice dimension lead to 6% T_1 underestimation.

Conclusion: The MS-MP2RAGE sequence could be used for fast whole body T_1 mapping and MR thermometry. Its reconstruction method would enable on-the-fly reconstruction.

Keywords: MP2RAGE, 2D Multi-slice, T1 mapping, mouse, Thermometry, 7T

Introduction

The Magnetization Prepared 2 Rapid Acquisition Gradient Echoes (MP2RAGE) sequence was initially developed for 3D acquisitions (1). It has been used for brain T_1 mapping in humans (1–3) and small-animals (4,5), at 3T and 7T. Its combination with Compressed Sensing (4) or Echo Planar (EPI) encoding has enabled faster acquisitions for instance whole human brain mapping in approximately 3 min (6). In parallel, its implementation with radial encoding has been used for mouse abdominal T_1 maps, with high robustness to motion and to acceleration using under-sampling (7). Nevertheless, because of its 3D encoding, the acquisition time is still too long for routine use.

To date, 2D encoding remains the reference method for fast and ultra-fast imaging. It has also regained interest since the development of Simultaneous Multi-Slice technique (8). For parametric T_1 mapping, sequences based on the Look-Locker scheme (9) or fingerprinting (10) have been employed. However, long acquisition times or high computational requirements, especially in signal post-processing, are needed. One of the fastest and most widely used T_1 mapping method is the Variable Flip Angle (VFA) (11,12). The latter requires at least 2 images at different nutation angles. Also, a steady state needs to be reached before data acquisition. Multiple angles may also have to be employed to measure a wide range of T_1 . Finally, this approach is very sensitive to the nutation angle (13), thus preventing fast and robust 2D T_1 mapping.

In regard to these different approaches, there is still a need for developing a fast and robust T_1 mapping method that can be applied to multiple areas of the body, and for numerous purposes, like diagnosis and monitoring of lesions or guiding interventional procedures. Indeed, quantitative T_1 values can be used in numerous pathologies as a diagnostic or prognostic tool (14–16). It can also be useful in interventional MRI, as a surrogate to PRF thermometry either in lipid (17,18) or bone (19) or in areas affected by respiration which can induce large changes in the phase (20).

Thus, the goal of this study is to develop a 2D MP2RAGE sequence to rapidly acquire T_1 maps with fast reconstruction. To further improve the pulse sequence efficiency, the multiple dead times within the chronogram were used for the acquisition of multiple 2D slices, leading to 6 T_1 maps achieved in 9s. The current study evaluates the versatility of a new 2D Multi-Slice MP2RAGE (MS-MP2RAGE) sequence, in two different contexts (i) as a

1
2
3 proof of concept on phantoms for MR thermometry and (ii) for in vivo fast T_1 mapping of
4 mouse brain and abdomen.
5
6
7

8 **Methods**

9 *MRI system*

10 Experiments were performed on a 7T Bruker BioSpec system equipped with a gradient
11 coil of 660 mT m^{-1} maximum strength and $110 \mu\text{s}$ rise time. A transmit volume resonator
12 operating in quadrature mode (75.4 mm inner diameter, 70 mm active length), and a
13 receive proton phased array (RAPID Biomedical GmbH – 4 elements of 30 mm long
14 around an elliptic cylinder housing: $19 \times 25.5 \text{ mm}$) were used.
15
16
17
18
19

20 For temperature monitoring experiments, the volume resonator was used in transmit and
21 receive mode.
22
23
24
25

26 T_1 maps were reconstructed using MATLAB (Mathworks, Natick, MA) with gpuNUFFT
27 (21) on a workstation containing two Xeon E5-2620 v4 processors (2.10 GHz, 8 cores,
28 INTEL Santa Clara, California) with 32 GB RAM and a Quadro M5000 Graphic Processing
29 Unit (GPU) card (8 GB RAM, NVIDIA, Santa Clara, California).
30
31
32
33
34

35 *2D Multi-Slice radial MP2RAGE sequence development*

36 The MS-MP2RAGE sequence was developed with a golden-angle radial encoding scheme.
37 As for the 3D Cartesian (1) and radial (7) MP2RAGE sequences, the selective inversion
38 pulse was followed by two gradient echo blocks (GRE1 and GRE2) acquired at two
39 different inversion times (TI_1 and TI_2 , respectively). The sequence repetition time was
40 referred to as $MP2RAGE_{TR}$.
41
42
43
44
45
46

47 In order to measure T_1 values between 500 and 2500 ms, TI_1 - TI_2 - $MP2RAGE_{TR}$ parameters
48 were set at 1000-3000-9000 ms. The reception bandwidth was set at 100 kHz (781
49 Hz/pixel) to get a TR of 5 ms within each GRE block. To avoid signal contamination from
50 the successive echoes, gradient spoilers were applied during the last millisecond. Thus,
51 the GRE blocks – containing 128 echoes – lasted 640 ms.
52
53
54
55
56
57
58
59
60

1
2
3 As selective pulses were used, the delays present in the MP2RAGE sequence could be used
4 to acquire five other slices (Figure 1). Slices were interleaved to prevent inversion slabs
5 overlap.
6
7

8 Overall, the delay between an inversion and the corresponding GRE1 was sufficient to
9 acquire a GRE block from another slice. Also, the delay between GRE1 and GRE2 was long
10 enough to acquire two GRE blocks from other slices. More precisely, the GRE1 blocks of
11 Slices 3 and 5 were acquired between the GRE1 and GRE2 of Slice 1. The corresponding
12 inversions were performed directly before the GRE1 of Slices 1 and 3, respectively. As a
13 consequence, the GRE2 blocks of Slices 3 and 5 were acquired after the GRE2 of Slice 1.
14 A dead time of 4.5 s remained after the GRE2 of Slice 5 for magnetization recovery. Thus,
15 another set of three intricate slices (Slices 2, 4 and 6) was acquired during this delay. To
16 reduce acquisition time, the inversion of Slice 2 was performed before the GRE2 of Slice 5.
17
18
19
20
21
22
23
24
25

26 As a result, the MS-MP2RAGE sequence enables to simultaneously acquire T_1 maps of 6
27 slices within 9 seconds. A set of six T_1 maps was reconstructed in less than 2 seconds.
28
29
30

31 *Phantom imaging*

32 To measure the performance of the MS-MP2RAGE sequence, T_1 maps were acquired on
33 five tubes with increasing T_1 values, on five different days, at room temperature ($25 \pm 2^\circ\text{C}$).
34 The tubes were prepared with saline and gadoteridol (ProHance®, Bracco imaging)
35 concentrated at 45, 75, 100, 135, and 215 μM to obtain T_1 values from 800 to 2000 ms.
36
37
38
39
40
41

42 The reference T_1 values and inversion efficiencies were determined via a gold standard
43 Inversion-Recovery (IR) sequence: Inversion pulse: 10-ms adiabatic hyperbolic secant
44 applied on 1250% of the imaging slice thickness; 120 TI from 100 to 12000ms (100ms
45 increment), TE = 10 ms, TR = 15 s, FOV = $25 \times 18 \text{ mm}^2$, matrix = 128×64 , resolution = 195
46 $\times 281 \mu\text{m}^2$, 1 slice, thickness = 2 mm, RARE Factor = 4; scan time ≈ 8 h.
47
48
49

50 Also, the 3D radial MP2RAGE (7) was performed on these phantoms, using the following
51 parameters: Inversion pulse: 10-ms adiabatic hyperbolic secant applied on 150% of the
52 imaging slab; T_{I_1} - T_{I_2} -MP2RAGE_{TR} = 1000/3000/9000ms; 0.25ms-hermite pulse; $\alpha_1 = \alpha_2$
53 = 7° ; TR = 5ms; 128 repetitions; FOV = $(25 \text{ mm})^3$, matrix = $(128)^3$, resolution = $(195 \mu\text{m})^3$.
54
55
56
57
58
59
60

1
2
3 The MS-MP2RAGE acquisitions were performed using the following parameters: FOV =
4 (25 mm)², matrix = (128)², resolution = (195 μm)², 1mm slice thickness.

5
6 The same excitation pulse was used in both GRE blocks ($\alpha_1 = \alpha_2 = 7^\circ$, 21.6 kHz
7 transmission bandwidth). Three different excitation pulse shapes were tested: 3 lobes
8 cardinal sine (sinc3), Hermitian and Gaussian. The transmission bandwidth being
9 constant, the pulse durations were 0.64, 0.25 and 0.13 ms, respectively. The
10 corresponding frequential excitation profiles are shown in Supporting Information Figure
11 S1a. Because low flip angles were used, the different excitation profiles had only low
12 influence on the signal – thus on the T_1 measurements (Supporting Information Figure
13 S1b).

14
15 Slab-selective inversions were performed using a 10-ms adiabatic hyperbolic secant
16 pulse. Because long MP2RAGE_{TR} were used, the steady-state magnetization (directly
17 before an inversion) and the equilibrium magnetization were similar (less than 1%
18 difference). Therefore, for each MP2RAGE_{TR}, the lookup table specifically developed for
19 radial encoding ((7); Supporting Information S1c) was used to measure T_1 (no dummy
20 scan was used).

21 22 23 24 25 26 27 28 29 30 31 32 33 *Inversion and slice gap influences*

34 To study the effect of the selective inversion on T_1 accuracy, the sequence was performed
35 with a single slice. Different inversion slabs covering 100, 125, 150, 175, 200 and 1000 %
36 of the imaging slice thickness were used in combination with the three excitation pulses
37 (sinc3, Hermitian and Gaussian) within the GRE blocks.

38
39 The influence of the gap separating the six slices was studied by increasing it from 0 to 25,
40 50 and 100% of the imaging slice thickness (*ie* 0, 0.25, 0.5 and 1 mm, respectively for a
41 1mm imaging slice).

42 43 44 45 46 47 48 49 50 51 *MR thermometry using the MS-MP2RAGE sequence*

52 Three tubes containing agarose gels (1% in saline) with gadoteridol at 75, 135 and
53 300 μM were prepared. To regulate their temperature inside the MRI scanner, the tubes
54 were placed in a home-made 3D-printed water circulation system: the system
55 temperature was controlled using circulating water, the water being heated in a bath
56 placed outside of the magnet room. An optical thermic probe (Luxtron 812, LumaSense
57
58
59
60

1
2
3 Technologies Inc., Santa Clara, USA) was inserted into a fourth tube containing only
4 agarose gel.
5
6
7

8 The temperature was recorded as the tubes were heated from 10 to 60°C. During this
9 time, 600 repetitions of the MS-MP2RAGE sequence were performed. The sequence
10 parameters were: inversion slab coverage of 150%, sinc3 excitation pulse, in-plane spatial
11 resolution $(312\mu\text{m})^2$, FOV = $(30\text{mm})^2$, matrix = 96^2 , slice thickness = 3mm, 50% inter-slice
12 gap = 1.5mm. An axial orientation was used to measure the T_1 of the three tubes
13 simultaneously. The acquisition lasted 1 h 30 min. This experiment was independently
14 performed four times.
15
16
17
18
19

20 The 3D radial MP2RAGE (7) was also performed at 10°C and 44°C, using the following
21 parameters: Inversion pulse: 10-ms adiabatic hyperbolic secant applied on 1000% of the
22 imaging slab; T_{I_1} - T_{I_2} -MP2RAGE_{TR} = 1000/3000/9000ms; 1ms-sinc10H pulse; $\alpha_1 = \alpha_2 = 7^\circ$;
23 TR=5ms; 128 repetitions; FOV = $(25\text{ mm})^3$, matrix = $(128)^3$, resolution = $(195\ \mu\text{m})^3$.
24
25
26
27
28
29

30 As a linear increase of T_1 with temperature was observed, the T_1 could be approximated
31 as $T_1 = T_1^0 + AT$, where both the slope A and the T_1 extrapolated at 0°C (T_1^0) are empirical
32 constants, while T is the temperature in Celcius. Both constants (T_1^0 and A) were
33 determined by linear regression and averaged over three experiments.
34
35

36 For the two tubes with the highest gadolinium (Gd) concentrations, all measurements
37 (from 10 to 60°C) were taken into account. However, for the third tube (75 μM), the T_1
38 above 40°C became too long to be measured with the current MP2RAGE parameters
39 ($>2500\text{ms}$). Therefore, in this case, only the measurements acquired between 10 and
40 40 °C were used.
41
42
43
44

45 The accuracy and precision of the temperature measurements were evaluated on each of
46 the three tubes:
47

- 48 - To evaluate accuracy, temperature deviations were calculated: the difference
49 between the temperature estimations (based on MS-MP2RAGE T_1 maps) and
50 reference temperatures (from the probe) were measured for the 600 repetitions.
51 The temperature bias was estimated as the mean over the 600 deviation values.
52 To determine the uncertainty, the corresponding standard deviation was
53 calculated.
54
55
56
57
58
59
60

- 1
2
3 - To evaluate the precision, the differences between two successive temperature
4 deviations were computed. The standard deviation over the 599 differences was
5 then calculated.
6
7
8
9

10 The T_1 Temperature Dependence Coefficient (TDC) of each tube was determined by
11 dividing the mean slope by the corresponding T_1 value measured at 30°C as already
12 performed by Kuroda *et al.* (22).
13
14
15

16
17 To evaluate the ability to monitor temperature in adipose tissues, the same experiment
18 was conducted three times on three identical tubes filled with olive oil.
19
20

21 22 *In vivo imaging*

23 The brain and abdomen of C57/Bl6 female mice (8 weeks old, Charles River, Labresle,
24 France) were scanned using the MS-MP2RAGE sequence. Three mice were used for each
25 body region. Similar parameters as for temperature imaging were used, except for the
26 slice thickness, which was set at 1.5 mm, and the 50% inter-slice gap set at 0.75mm. 200
27 repetitions were applied continuously, for a total exam time of 30 min.
28
29

30 The IR sequence previously described for phantom imaging was also applied on the brain
31 of three other healthy mice. The same parameters were used, except: 25 TI from 10 ms to
32 11900 ms, TR = 12 s, scan time = 2h.
33
34
35

36 The experimental procedures were approved by the Animal Care and Use Institutional
37 ethics committee of Bordeaux, France (approval no. APAFiS 2629-2015110618597936).
38
39
40

41 42 *Data analysis*

43 To obtain reference T_1 values and inversion efficiencies (named “eff”) from the IR
44 sequence, the signal of each of the five Gd-containing tubes was fitted using the equation
45 (23):
46
47

$$48 \quad y = \text{abs}(M_0 \times (1 - (1 + \text{eff}) \times \exp(-x/T_1))) \quad \text{Eq [1].}$$

49 A reference T_1 value was calculated as the mean T_1 measured with the gold-standard IR
50 sequence over the five experiments. The corresponding standard deviation was
51 calculated. “eff” was measured at $\approx 100\%$. Consequently, the MP2RAGE signal equation
52
53
54
55
56
57
58
59
60

was performed using $\text{eff}=100\%$, when reconstructing the subsequent MS-MP2RAGE and 3D MP2RAGE images.

The influence of the inversion selectivity and the excitation pulse profile were assessed on single slice MP2RAGE measurements. For each of the five tubes, the differences between the T_1 values obtained with the MP2RAGE and IR sequences were calculated. These differences were averaged over the five experiments and expressed as a percentage of the corresponding reference T_1 value of each tube. Finally, all these relative T_1 differences were averaged over the five tubes and the corresponding standard deviation was calculated.

The influence of the gap between imaging slices was measured for the tube with the longest T_1 (*ie* 75 μM). The T_1 of each slice was independently averaged over five experiments. The mean T_1 and corresponding standard deviation were calculated over the six slices.

To measure the precision and accuracy of the sequence after optimization of the parameters, the mean T_1 over the six slices was calculated and averaged over five experiments. The corresponding standard deviation and relative difference with the reference T_1 (obtained with the IR sequence) and with the 3D radial MP2RAGE were calculated. In addition, to assess the T_1 variation between slices (named Slice STDEV in Table 1), the standard deviation of the T_1 measured in the six slices were averaged over five experiments.

To measure T_1 of the mouse brain cortex and mi-brain with the IR sequence, the signals were fitted using a mono or a bi-exponential equation:

$$y = \text{abs}(M_{0,L} \times (1+\text{eff}) \times \exp(-x/T_{1,L}) + M_{0,S} \times (1+\text{eff}) \times \exp(-x/T_{1,S})) \quad \text{Eq [2],}$$

where L and S stand for “Long T_1 ” and “Short T_1 ” components, and eff stands for inversion efficiency.

To quantify the stability of the T_1 measurements obtained with the MS-MP2RAGE sequence run continuously for 30-min, Regions of Interest (ROI) were drawn in the liver (in two different slices), in the back muscle, in the midbrain and brain cortex. The mean T_1 of each of these ROI was displayed as a function of exam time. The temporal coefficient

of variation (COV) was calculated by dividing the temporal standard deviation of T_1 during the 30-min scan by its mean.

Results

Impact of the spatial selectivity of the inversion pulse on the T_1 measurements

When increasing the inversion slab coverage, the T_1 values tend to reach a plateau (Figure 2a). When a sinc3 pulse is used, this plateau is reached as soon as the inversion slab covered 150% of the excitation slice thickness. However, with the other pulses (Hermitian and Gaussian), a minimum thickness of 175% or >200% was necessary to reach the reference T_1 value, respectively. Therefore, the combination of a sinc3 excitation pulse and a 150% inversion slab was used for the MS-MP2RAGE experiments thereafter.

Impact of the excitation slice gap on the T_1 measurements

Figure 2b) shows the influence of the gap between the 6 imaging slices on the T_1 measurements (with 150% inversion slab). Even though slice acquisitions were interlaced, the T_1 values were affected when the slices were adjacent (0%-gap): the T_1 values were under-estimated by up to 10% and a high T_1 standard deviation was measured over the six slices. Increasing the gap to half the width of the imaging slice (50%-gap) allowed to obtain similar T_1 measurements on all the 6 slices. T_1 measurements obtained with a 100%-gap were similar to those with a 50%-gap. In order to maintain fine characterization of the sample of interest, a 50%-gap was set for the following experiments.

Measurement accuracy

A wide range of T_1 values (800 to 2000 ms) was assessed using the MS-MP2RAGE sequence with the parameters optimized above (150% selective inversion, sinc3 excitation pulses, 50% inter-slice-gap), the 3D radial MP2RAGE and the standard IR sequence (Table 1). The comparison between the sequences shows T_1 differences below 5%.

MR thermometry using T_1 measurement

1
2
3 The fast acquisition strategy developed here enabled to apply the MS-MP2RAGE sequence
4 for MR thermometry. The T_1 maps acquired every 9 s enabled to observe a linear increase
5 of the T_1 with temperature for the three Gd concentrations tested (Figure 3).

6
7
8 The 3D radial MP2RAGE sequence applied at two temperatures (10°C and 44°C)
9 demonstrated less than 5% differences in T_1 values compared to the ones obtained with
10 the MS-MP2RAGE sequence. This implies a minimum effect of Diffusion in our set up.

11
12 For the 75, 135 and 300 μM tubes, the corresponding slopes (A) were measured at 39 ± 2 ,
13 27 ± 1 and 21 ± 3 $\text{ms } ^\circ\text{C}^{-1}$, respectively. The corresponding T_1 interpolated at 0°C (T_1^0) were
14 estimated at 780 ± 20 , 410 ± 40 and 290 ± 60 ms, respectively.
15
16
17
18
19

20
21 From these empirical constants (A and T_1^0), temperatures from 10 to 60 °C were predicted
22 based on the T_1 values measured with the MS-MP2RAGE sequence (Figure 4). For the tube
23 containing 75 μM of Gd, T_1 got too long (above 2500ms) to be measured with the current
24 parameters at high temperatures.
25
26
27

28 Temperature biases of 1.7 ± 0.5 , 0.0 ± 1.0 and 3.0 ± 0.9 °C with corresponding precisions of
29 ± 0.5 , ± 1.0 and ± 0.7 °C were measured for the 75, 135 and 300 μM tubes, respectively.
30
31
32

33 Globally, a T_1 TDC of 2.2 ± 0.2 %/°C was measured at 30°C on the three tubes.
34
35

36
37 In tubes filled with olive oil, T_1 values from 300 to 600 ms were measured over the 10 to
38 60°C elevation (data not shown). A mean slope of 2.4 ± 0.9 $\text{ms} \cdot ^\circ\text{C}^{-1}$ was measured (*ie* 26%
39 uncertainty on the slope); the mean T_1^0 was 427 ± 7 ms.
40
41
42
43

44 *In vivo measurement*

45 Using the IR sequence, a short T_1 component ($T_{1,s} \approx 95\text{ms}$) could be measured using a bi-
46 exponential fit (Supporting Information Table S1). This component can generate up to
47 5%-underestimations of $T_{1,L}$ when fitting the data with a mono-exponential equation.
48 Also, the data enabled to measure the inversion efficiency (eff) on the mouse brain at 93%
49 $\pm 3\%$. Consequently, this value was used into the MP2RAGE signal equations. The
50 corresponding T_1 measurements obtained with the MS-MP2RAGE sequence lengthened
51 by 5% and 4.3% in the cortex and mid-brain, respectively.
52
53
54
55
56
57
58
59
60

1
2
3 The MS-MP2RAGE sequence was then applied on mice. In the brain (Figure 5a, upper
4 row), T_1 standard deviations of 8 ms were measured along a 30-min acquisition (*ie* 200
5 repetitions) corresponding to a COV of less than 1% (Figure 5b).
6
7

8 The sequence was then used for mouse abdominal imaging while free breathing
9 (Figure 5a, lower row). Due to the radial encoding, respiratory motion did not result in
10 obvious in-plane motion artifacts. Due to the large reception bandwidth used here, no
11 chemical shift was observed. The standard deviation measured in a ROI drawn inside the
12 liver was 60 ms corresponding to a COV of 6%, over 200 repetitions. Similar standard
13 deviations were observed on a second slice in the liver, yet the mean T_1 was slightly
14 different between the two slices (921 ± 57 and 890 ± 60 ms, respectively, Figure 5b). Over
15 a 30-min acquisition, low T_1 standard deviation was measured in the back muscle (15 ms,
16 *i.e.* COV= 1%).
17
18
19
20
21
22
23
24
25

26 Discussion

27 This paper demonstrates the possibility to obtain accurate T_1 maps with a 2D
28 implementation of the radial MP2RAGE sequence (1,7). The main advantages of the
29 current approach rely on its broad applicability, rapid acquisition scheme, and its
30 simplicity in image reconstruction. In comparison, VFA methods require 3D
31 implementations (13) and are less robust to B_1 than the MP2RAGE sequence. Look-Locker
32 and Fingerprinting sequences demand high computational requirements for generating
33 the T_1 maps. Compared to 3D MP2RAGE approaches (4,6), the 2D encoding scheme
34 drastically reduced the scan time of the MP2RAGE sequence, while maintaining accurate
35 T_1 measurements. To further accelerate, using selective pulses, the dead times of the
36 MP2RAGE sequence were used to acquire multiple slices. This resulted in a compact and
37 fast T_1 mapping sequence, with the possibility to acquire 6 slices in 9 seconds. Despite this
38 encoding strategy, the Specific Absorption Rate (SAR) of this sequence was estimated at
39 $< 0.5W/kg$, which is well below the recommended values. Thus, translating this sequence
40 into a routine protocol in clinics is feasible. Yet, 2D imaging has also some specific
41 requirements. To prevent parasite signal from spins outside the inversion slab –
42 especially when using Hermitian and Gaussian pulses – the inversion selectivity needed
43 to be adapted, which in turn conditioned the size of the inter-slice gap. A way of reducing
44 this gap would be to improve pulse selectivity while maintaining a short TR. Apodization
45 function (24) or Variable-Rate Selective Excitation (VERSE) (25,26) could be used.
46
47
48
49
50
51
52
53
54
55
56
57
58
59
60

Application for fast in vivo mapping

Fast T_1 mapping of the whole mouse brain with the MS-MP2RAGE sequence showed the ability to measure T_1 values with low variations along time (less than 1%). The in vivo T_1 values measured with the MS-MP2RAGE sequence had to be corrected for the inversion efficiency, leading to values within the range found in the existing literature (4,27–30). This study highlights the potential of this sequence to be used during longitudinal studies. Still, Magnetization Transfer effect (31) and T2 decay during the long inversion pulse (32,33) might explain the remaining <15% T_1 differences with a IR sequence. Nevertheless, in the liver, after correction of the inversion efficiency, the mean T_1 values measured with the MS-MP2RAGE sequence were in agreement with those found in the literature (7,16). Variability in T_1 standard deviations can be due to respiration motion, which could prevent a perfect overlap between inversion slabs and imaging slices. Another source of T_1 errors might come from motion between the acquisitions of the GRE1 and GRE2 blocks of the same slice, which may be corrected through the deletion of motion-corrupted projections identified by a self-gating method (34). Another solution would be to perform 9-seconds apnea, which can be easily implemented on humans. Another way to improve the robustness to motion, is to use less-selective inversions, that would require increasing the inter-slice gap. To counteract this decrease in spatial resolution in the slice direction, a solution would be to increase the gap to 100%, and acquire missing slices in a second set of six slices within another MS-MP2RAGE_{TR} (thus 12 adjacent slices could be acquired in 18 s). In that case, one set of six slices should be acquired in a sequential mode (rather than interlaced), which will not affect the T_1 values of the next slice set. The compatibility of the sequential mode with 100%-gap is illustrated in Supporting Information Table S2.

Application to thermometry

One application of the fast T_1 mapping obtained with the MS-MP2RAGE sequence is temperature monitoring. At 7T, there is a lack of literature concerning tissue T_1 variations with temperature. Nevertheless, the slopes obtained in our study are close to those obtained in the literature at 3T in breast aqueous tissues (35) or in fat (17,22). According to our data, a precision of $\pm 1^\circ\text{C}$ was feasible in aqueous tissues that were not corrupted

1
2
3 by motion. Yet, a low temperature accuracy was observed that could be due to lack of
4 accuracy and precision when determining empirical constants (A and T_1^0) from the small
5 sample size, as well as difficulties to replicate the phantoms and variations in the probe
6 location within the 3 mm imaging slice.
7
8
9

10
11 Using the current MS-MP2RAGE parameters, a wide range of T_1 values were measured.
12 This is an advantage compared to VFA-based thermometry, which requires specific flip
13 angles to accurately measure a small range of T_1 values. A minor drawback with our
14 current sequence was that T_1 longer than 2500 ms could not be measured. In the
15 perspective of translating the sequence into a temperature monitoring protocol, this
16 might not be a limiting factor. Indeed, at 3T, from the empirical constants (A and T_1^0)
17 determined from Birkl et al (36) on the brain cortex – which has one of the longest T_1
18 values in the brain (1) – a T_1 of approximately 2000 ms was simulated at 60 °C. Still, if
19 there is a need for measuring >2500 ms T_1 values, the sequence parameters could be
20 adapted. TI_1 , TI_2 and $MP2RAGE_{TR}$ could be lengthened while affecting the temporal
21 resolution or the flip angle could be increased (Supporting Information Figure S1c) which
22 in that case might require B_1 correction.
23
24
25
26
27
28
29
30
31
32
33

34
35 One advantage of T_1 mapping versus PRF methods is the possibility to measure
36 temperature variations in adipose tissues, or bones using a UTE encoding scheme (19,37).
37 In oil, the T_1 measured in the current study at 20°C is close to the value measured in
38 hypodermis (fat) by Barral *et al* at the same temperature at 7T (38) – despite a difference
39 in sample characteristics. The T_1 -Temperature slope measured with the MS-MP2RAGE
40 sequence was low compared to the one measured at 3T by Todd *et al* (17); the large slope
41 variation could be explained by the proximity of the T_1 value of oil from the lower bound
42 of the MP2RAGE lookup table. To circumvent this issue, the TI_1 could be reduced to 800
43 ms. This would imply reducing the number of projections per GRE to 100, which could be
44 compensated using either k-Space Weighted Image Contrast (KWIC) (39) or Compressed
45 Sensing (CS) (4,40,41). Still, if fat is the tissue of interest, TI_2 and $MP2RAGE_{TR}$ could also
46 be reduced to 2400 and 7000 ms, respectively, which would improve the temporal
47 resolution. Thus, T_1 values could be measured between 400 and 2000 ms rather than
48 between 500 and 2500 ms, as in the current study.
49
50
51
52
53
54
55
56
57
58
59
60

Limitations for thermometry applications

As already demonstrated, T_1 mapping cannot be used to measure absolute temperature, due to tissue-dependent T_1 -Temperature evolutions. To further develop the MS-MP2RAGE sequence as a temperature monitoring protocol, calibration studies can be performed to characterize the T_1 -Temperature dependence of the tissue of interest. PRF information might also be necessary. Several publications have already developed MR sequences in order to simultaneously obtain PRF and T_1 measurements (17,18,35,42–44). Due to a radial encoding similar to the one implemented here and the use of a KWIC filter, 3D PRF and T_1 maps were obtained extremely rapidly (45). Nevertheless, the implementation and the process for image reconstruction could be difficult to operate in routine. To obtain both information with the MS-MP2RAGE sequence, the TE of the GRE can be lengthened to get closer to the optimal condition $TE=T_2^*$. Nevertheless, a longer TE would generate a longer echo train than the current sequence, which would either limit the use of the Multi-Slice acquisition developed here, or decrease the spatial resolution of the T_1 maps due to the reduction in the number of echoes per train.

Perspectives

In MR thermometry, fast acquisitions have to be coupled to fast image reconstruction. Here, a set of 6 slices was reconstructed in less than 2 seconds. To further accelerate this reconstruction, one of our future directions is to implement the open-source Gadgetron software (46,47) to dynamically modify the sequence parameters along with the temperature elevation.

Another perspective would be to use acceleration methods to acquire more slices in a single MP2RAGE_{TR}. For instance, the GRE length could be shortened using under-sampling; KWIC (39) or CS (4,40,41) could then be used to reduce aliasing artifacts. Parallel imaging would also enable simultaneous multi-slice acquisition (48,49), thus extending applications of the MS-MP2RAGE sequence to whole-body T_1 mapping.

It would also be possible to replace the radial encoding scheme by a Cartesian one to get better resolution in the absence of motion, or to implement an Ultra-short Echo Time (UTE) encoding to measure T_1 in short T_2^* environments.

Conclusion

The MS-MP2RAGE sequence has shown to be an efficient method to rapidly acquire 2D T_1 maps, which has a potential for 'on-the-fly' reconstruction. Depending on the application, the pulse sequence could be combined with different encoding schemes and acceleration methods.

Acknowledgment

This study was achieved within the context of the Laboratory of Excellence TRAIL ANR-10-LABX-57. The authors thank Dr N. Koonjoo for English editing.

References

1. Marques JP, Kober T, Krueger G, van der Zwaag W, Van de Moortele P-F, Gruetter R. MP2RAGE, a self bias-field corrected sequence for improved segmentation and T_1 -mapping at high field. *Neuroimage* 2010;49:1271–1281.
2. Marques JP, Gruetter R. New Developments and Applications of the MP2RAGE Sequence - Focusing the Contrast and High Spatial Resolution R_1 Mapping Yacoub E, editor. *PLoS One* 2013;8:e69294 doi: 10.1371/journal.pone.0069294.
3. Hagberg GE, Bause J, Ethofer T, et al. Whole brain MP2RAGE-based mapping of the longitudinal relaxation time at 9.4T. *Neuroimage* 2017;144:203–216.
4. Trotier AJ, Rapacchi S, Faller TL, Miraux S, Ribot EJ. Compressed-Sensing MP2RAGE sequence: Application to the detection of brain metastases in mice at 7T. *Magn. Reson. Med.* 2019;81:551–559.
5. Driencourt L, Romero CJ, Lepore M, Eggenschwiler F, Reynaud O, Just N. T_1 mapping of the mouse brain following fractionated manganese administration using MP2RAGE. *Brain Struct. Funct.* 2017;222:201–214.
6. van der Zwaag W, Buur PF, Fracasso A, et al. Distortion-matched T_1 maps and unbiased T_1 -weighted images as anatomical reference for high-resolution fMRI. *Neuroimage* 2018;176:41–55.
7. Faller TL, Trotier AJ, Miraux S, Ribot EJ. Radial MP2RAGE sequence for rapid 3D T_1 mapping of mouse abdomen: application to hepatic metastases. *Eur. Radiol.* 2019 doi: 10.1007/s00330-019-06081-3.
8. Barth M, Breuer F, Koopmans PJ, Norris DG, Poser BA. Simultaneous multislice (SMS) imaging techniques. *Magn. Reson. Med.* 2016;75:63–81.
9. Ehses P, Seiberlich N, Ma D, et al. IR TrueFISP with a golden-ratio-based radial readout:

- 1
2
3 fast quantification of T1, T2, and proton density. *Magn. Reson. Med.* 2013;69:71–81.
- 4
5 10. Jiang Y, Ma D, Seiberlich N, Gulani V, Griswold MA. MR fingerprinting using fast
6
7 imaging with steady state precession (FISP) with spiral readout. *Magn. Reson. Med.*
8
9 2015;74:1621–1631.
- 10
11 11. Deoni SCL, Rutt BK, Peters TM. Rapid combined T1 and T2 mapping using gradient
12
13 recalled acquisition in the steady state. *Magn. Reson. Med.* 2003;49:515–526.
- 14
15 12. Cheng H-LM, Wright GA. Rapid high-resolution T1 mapping by variable flip angles:
16
17 Accurate and precise measurements in the presence of radiofrequency field
18
19 inhomogeneity. *Magn. Reson. Med.* 2006;55:566–574.
- 20
21 13. Svedin BT, Parker DL. Technical Note: The effect of 2D excitation profile on T1
22
23 measurement accuracy using the variable flip angle method with an average flip angle
24
25 assumption. *Med. Phys.* 2017;44:5930–5937.
- 26
27 14. Weidensteiner C, Allegrini PR, Sticker-Jantscheff M, Romanet V, Ferretti S, McSheehy
28
29 PM. Tumour T1 changes in vivo are highly predictive of response to chemotherapy and
30
31 reflect the number of viable tumour cells – a preclinical MR study in mice. *BMC Cancer*
32
33 2014;14:88.
- 34
35 15. Ravoori MK, Nishimura M, Singh SP, et al. Tumor T1 Relaxation Time for Assessing
36
37 Response to Bevacizumab Anti-Angiogenic Therapy in a Mouse Ovarian Cancer Model.
38
39 Kanthou C, editor. *PLoS One* 2015;10:e0131095 doi: 10.1371/journal.pone.0131095.
- 40
41 16. Chow AM, Gao DS, Fan SJ, et al. Measurement of liver T1 and T2 relaxation times in an
42
43 experimental mouse model of liver fibrosis. *J. Magn. Reson. Imaging* 2012;36:152–158.
- 44
45 17. Todd N, Diakite M, Payne A, Parker DL. Hybrid proton resonance frequency/T1
46
47 technique for simultaneous temperature monitoring in adipose and aqueous tissues.
48
49 *Magn. Reson. Med.* 2013;69:62–70 doi: 10.1002/mrm.24228.
- 50
51 18. Todd N, Diakite M, Payne A, Parker DL. In vivo evaluation of multi-echo hybrid PRF/T1
52
53 approach for temperature monitoring during breast MR-guided focused ultrasound
54
55 surgery treatments. *Magn. Reson. Med.* 2014;72:793–799.
- 56
57 19. Han M, Rieke V, Scott SJ, et al. Quantifying temperature-dependent T1 changes in
58
59 cortical bone using ultrashort echo-time MRI. *Magn. Reson. Med.* 2015;74:1548–1555.
- 60
61 20. Svedin BT, Payne A, Parker DL. Respiration artifact correction in three-dimensional
62
63 proton resonance frequency MR thermometry using phase navigators. *Magn. Reson. Med.*
64
65 2016;76:206–213.
- 66
67 21. Knoll F, Schwarzl A, Diwoký C, Sodickson D. *gpuNUFFT*-An open source GPU library

- 1
2
3 for 3 D regridding with direct Matlab interface. In Proceedings of the 22nd Annual
4 Meeting of ISMRM, Milan, IT; 2014. Abstract 4297.
- 5
6 22. Kuroda K, Iwabuchi T, Obara M, Honda M, Saito K, Imai Y. Temperature dependence
7 of relaxation times in proton components of fatty acids. *Magn. Reson. Med. Sci.*
8 2011;10:177–183.
- 9
10 23. Barral JK, Gudmundson E, Stikov N, Etezadi-Amoli M, Stoica P, Nishimura DG. A robust
11 methodology for in vivo T1 mapping. *Magn. Reson. Med.* 2010;64:1057–1067.
- 12
13 24. Park J, Park J-Y. A New Tailored Sinc Pulse and Its Use for Multiband Pulse Design.
14 *Investig. Magn. Reson. Imaging* 2016;20:27–35.
- 15
16 25. Conolly S, Nishimura D, Macovski A, Glover G. Variable-rate selective excitation. *J.*
17 *Magn. Reson.* 1988;78:440–458.
- 18
19 26. Lee D, Lustig M, Grissom WA, Pauly JM. Time-optimal design for multidimensional and
20 parallel transmit variable-rate selective excitation. *Magn. Reson. Med.* 2009;61:1471–
21 1479.
- 22
23 27. Castets CR, Koonjoo N, Hertanu A, et al. In vivo MEMRI characterization of brain
24 metastases using a 3D Look-Locker T1-mapping sequence. *Sci. Rep.* 2016;6:39449 doi:
25 10.1038/srep39449.
- 26
27 28. Guilfoyle DN, Dyakin V V, O’Shea J, Pell GS, Helpert JA. Quantitative measurements of
28 proton spin-lattice (T1) and spin-spin (T2) relaxation times in the mouse brain at 7.0 T.
29 *Magn. Reson. Med.* 2003;49:576–580.
- 30
31 29. Pohmann R, Shajan G, Balla DZ. Contrast at high field: Relaxation times, magnetization
32 transfer and phase in the rat brain at 16.4 T. *Magn. Reson. Med.* 2011;66:1572–1581.
- 33
34 30. Gao Y, Chen Y, Ma D, et al. Preclinical MR fingerprinting (MRF) at 7 T: effective
35 quantitative imaging for rodent disease models. *NMR Biomed.* 2015;28:384–394.
- 36
37 31. Rioux JA, Levesque IR, Rutt BK. Biexponential longitudinal relaxation in white matter:
38 Characterization and impact on T1 mapping with IR-FSE and MP2RAGE. *Magn. Reson.*
39 *Med.* 2016;75:2265–2277.
- 40
41 32. Norris DG, Lüdemann H, Leibfritz D. An analysis of the effects of short T2 values on the
42 hyperbolic-secant pulse. *J. Magn. Reson.* 1991;92:94–101.
- 43
44 33. Kellman P, Herzka DA, Hansen MS. Adiabatic inversion pulses for myocardial T1
45 mapping. *Magn. Reson. Med.* 2014;71:1428–1434.
- 46
47 34. Winter P, Kampf T, Helluy X, et al. Self-navigation under non-steady-state conditions:
48 Cardiac and respiratory self-gating of inversion recovery snapshot FLASH acquisitions in
49
50
51
52
53
54
55
56
57
58
59
60

1
2
3 mice. *Magn. Reson. Med.* 2016;76:1887–1894.

4
5 35. Svedin BT, Payne A, Parker DL. Simultaneous proton resonance frequency shift
6 thermometry and T₁ measurements using a single reference variable flip angle T₁
7 method. *Magn. Reson. Med.* 2019;81:3138–3152.

8
9
10 36. Birkl C, Langkammer C, Haybaeck J, et al. Temperature-induced changes of magnetic
11 resonance relaxation times in the human brain: A postmortem study. *Magn. Reson. Med.*
12 2014;71:1575–1580.

13
14 37. Du J, Bydder GM. Qualitative and quantitative ultrashort-TE MRI of cortical bone. *NMR*
15 *Biomed.* 2013;26:489–506.

16
17 38. Barral JK, Stikov N, Gudmundson E, Stoica P, Nishimura DG. Skin T₁ Mapping at 1.5T,
18 3T, and 7T. In *Proceedings of the 17th Annual Meeting of ISMRM, Honolulu, HI, 2009.*
19 Abstract 4451.

20
21 39. Song HK, Dougherty L. k-space weighted image contrast (KWIC) for contrast
22 manipulation in projection reconstruction MRI. *Magn. Reson. Med.* 2000;44:825–832.

23
24 40. Block KT, Uecker M, Frahm J. Undersampled radial MRI with multiple coils. Iterative
25 image reconstruction using a total variation constraint. *Magn. Reson. Med.*
26 2007;57:1086–1098.

27
28 41. Levine E, Daniel B, Vasanawala S, Hargreaves B, Saranathan M. 3D Cartesian MRI with
29 compressed sensing and variable view sharing using complementary poisson-disc
30 sampling. *Magn. Reson. Med.* 2017;77:1774–1785.

31
32 42. Hey S, de Smet M, Stehning C, et al. Simultaneous T₁ measurements and proton
33 resonance frequency shift based thermometry using variable flip angles. *Magn. Reson.*
34 *Med.* 2012;67:457–463.

35
36 43. Bos C, Lepetit-Coiffé M, Quesson B, Moonen CTW. Simultaneous monitoring of
37 temperature and T₁: Methods and preliminary results of application to drug delivery
38 using thermosensitive liposomes. *Magn. Reson. Med.* 2005;54:1020–1024.

39
40 44. Diakite M, Payne A, Todd N, Parker DL. Irreversible change in the T₁ temperature
41 dependence with thermal dose using the proton resonance frequency- T₁ technique.
42 *Magn. Reson. Med.* 2013;69:1122–1130.

43
44 45. Zhang L, Armstrong T, Li X, Wu HH. A variable flip angle golden-angle-ordered 3D
45 stack-of-radial MRI technique for simultaneous proton resonant frequency shift and T₁
46 -based thermometry. *Magn. Reson. Med.* 2019;82:2062–2076.

47
48 46. Hansen MS, Sørensen TS. Gadgetron: An open source framework for medical image
49
50
51
52
53
54
55
56
57
58
59
60

reconstruction. *Magn. Reson. Med.* 2013;69:1768–1776.

47. Ozenne V, Toupin S, Bour P, et al. Improved cardiac magnetic resonance thermometry and dosimetry for monitoring lesion formation during catheter ablation. *Magn. Reson. Med.* 2017;77:673–683.

48. Weingärtner S, Moeller S, Schmitter S, et al. Simultaneous multislice imaging for native myocardial T₁ mapping: Improved spatial coverage in a single breath-hold. *Magn. Reson. Med.* 2017;78:462–471.

49. Rapacchi S, Troalen T, Bentatou Z, et al. Simultaneous multi-slice cardiac cine with Fourier-encoded self-calibration at 7 Tesla. *Magn Reson Med.* 2019;81(4):2576- 2587.

Figure captions

Figure 1: Chronogram of the 2D MS-MP2RAGE sequence. In this implementation, the usual MP2RAGE delays – namely TI_1 , TI_2 and $MP2RAGE_{TR}$ – are respectively set to 1000, 3000 and 9000 ms. GRE blocks of 640 ms were set. Other delays are shown on the chronogram of Slice 3. The interleaving of the six slices is shown.

Figure 2: Impact of the inversion selectivity and inter-slice gap on the T₁ measurements. a) Relative T₁ difference (in percent) between MS-MP2RAGE and IR measurements using Gaussian (grey), Hermitian (hatch) or Cardinal sine (black) excitation pulses as a function of the inversion slab coverage (expressed in percentage of the 1-mm excitation slice thickness). b) T₁ measurements on six different slices located on the tube containing 75 μ M Gd ($T_1=1852$ ms measured by IR, dashed line), as a function of the gap between each slice. The gap was increased from 0% to 25%, 50% and 100%. For each slice, the mean T₁ over the five experiments is represented by a dot. For each gap, the mean T₁ (cross) and the corresponding error bar over all six slices are shown. The 1-mm slices were acquired with an interlaced scheme, using an inversion slab set at 150% and a sinc3 excitation pulse.

Figure 3: T₁ measurements while heating. a) Three representative axial T₁ maps (top) of agarose gels containing Gd at 75 (green), 135 (red) and 300 (blue) μ M acquired at three temperatures (10°C, 25°C and 40°C). The tube encircled in gray contains the temperature probe. b) Graph showing the T₁ measured in the three corresponding Gd-containing tubes as a function of the temperature measured with the probe. For each tube, the linear equation of T₁ dependence on temperature is calculated using linear regression.

Figure 4: Temperature monitoring. The mean slopes and intercept (A and T_1^0) were calculated over three experiments, and used to estimate temperature warming during an independent experiment. The temperatures were estimated within the three Gd-containing tubes 75 (green), 135 (red) and 300 (blue) μM in the slice at the location of the probe (black solid line). The circulating water was first warmed to 60°C for 50 minutes, then to 80°C for 40 minutes, explaining the inflexion around 50 minutes.

Figure 5: T_1 evolution in vivo over 30 minutes. a) Six axial T_1 maps of the brain (first row) and six coronal T_1 maps of the abdomen (second row) were acquired with 1-mm slice thickness, spaced by 0.5 mm. Each six slices set was acquired in 9 s, while free breathing. b) T_1 evolution in mouse back muscle (blue), in two slices containing the liver (red full and dashed lines), in the mouse midbrain (black dashed line) and brain cortex (black full line) are shown.

Table

Table 1: In vitro T_1 measurements obtained with the MS-MP2RAGE (sinc3 pulse, 150% selective inversion, 50% gap), the IR and the 3D radial MP2RAGE sequences. The differences (expressed in percentage of the corresponding T_1 value) between the MS-MP2RAGE and the IR sequences and between the MS-MP2RAGE and the 3D radial MP2RAGE sequences are shown.

[Gd] / μM	45	75	100	135	215
reference IR T_1 / ms	885 \pm 8.7	1058 \pm 29	1335 \pm 25	1568 \pm 89	1853 \pm 47
MS-MP2RAGE T_1 / ms (\pm Slice STDEV / ms)	891 \pm 21 (\pm 4.0)	1060 \pm 28 (\pm 6.9)	1340 \pm 27 (\pm 5.7)	1542 \pm 103 (\pm 8.4)	1851 \pm 32 (\pm 9.9)
MS-MP2RAGE vs IR / %	0.65	0.15	0.47	-1.6	-0.12
3D MP2RAGE T_1 / ms	931 \pm 28	1111 \pm 37	1384 \pm 25	1600 \pm 116	1903 \pm 39
MS-MP2RAGE vs 3D MP2RAGE / %	4.6	4.8	3.2	3.7	2.9

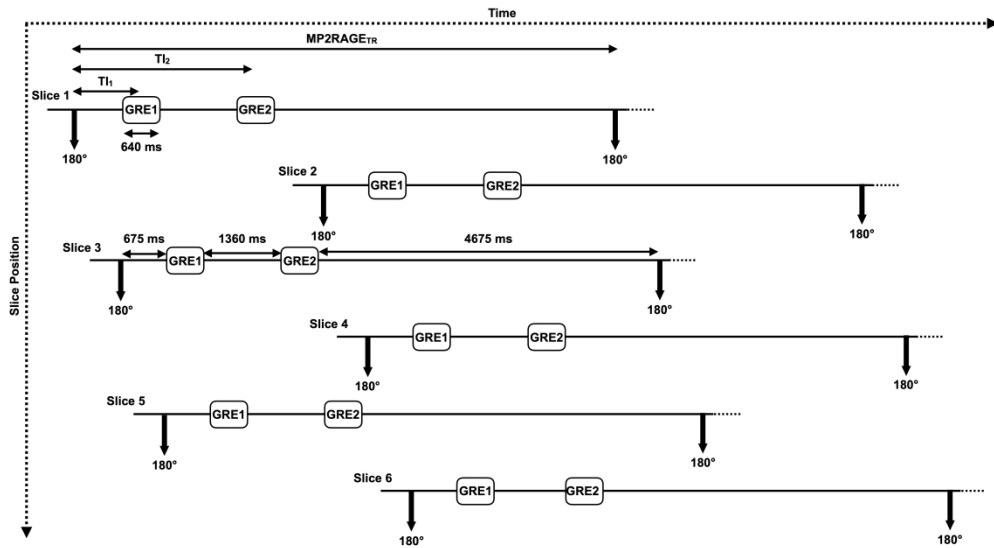
Supporting Information captions

Supporting Information Figure S1: Influence of the excitation pulse on T_1 measurements.

a) To assess the slice profiles of three different excitation pulses, simulations were performed over two bandwidths with 4320 points (2x21.6kHz, 100Hz resolution). Ideal slice: dashed line, Gaussian pulse (Time-Bandwidth Product (TBP)=2.74): red, Hermitian pulse (TBP=5.4): blue, Sinc3 pulse (TBP=6.21): yellow. The signal of one echo was then calculated, using Bloch equations, as the sum of the signal over the two bandwidths. b) The hypothesis of an ideal slice profile to compute the lookup table would lead to T_1 overestimations, depending on the T_1 . Still, as low flip-angles are usually used ($<7^\circ$), this overestimation is quite low: for Hermitian and sinc3 pulses, an overestimation of less than 2% is evaluated when T_1 is shorter than 2500ms. It is slightly less than doubled when using a Gaussian pulse, which has a lower Time-Bandwidth Product (2.74 against 5.4 and 6.21 for the sinc3 and Hermitian, respectively). c) Simulation of lookup tables computed with different flip angles (blue: 1° , red: 4° , yellow: 7° , purple: 10° , green: 13°).

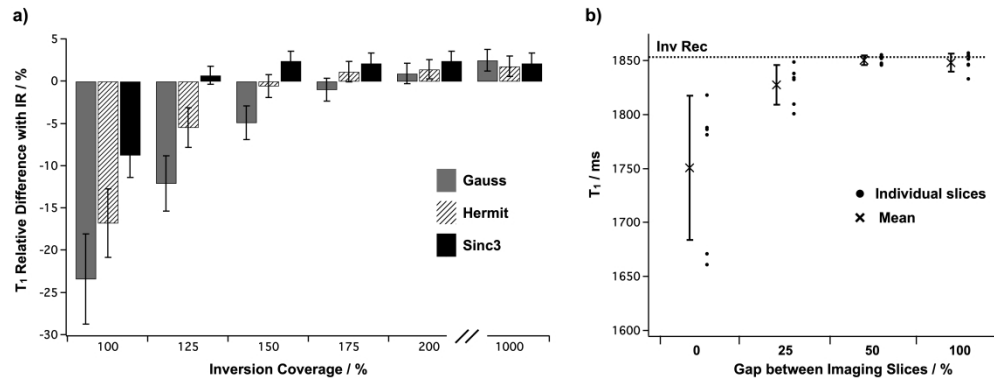
Supporting Information Table S1: Mouse brain T_1 measurements using the IR sequence and two different fit equations (mono- or bi-exponential). The inversion efficiencies (eff), the short and long T_1 component ($T_{1,S}$ and $T_{1,L}$, respectively), and the ratio $M_{0,S}/M_{0,L}$ are shown for two brain regions (cortex and mid-brain).

Supporting Information Table S2: T_1 measurements using the MS-MP2RAGE in a sequential mode (with 100%-gap) and the IR sequence on the 75 μM Gd-containing tube.



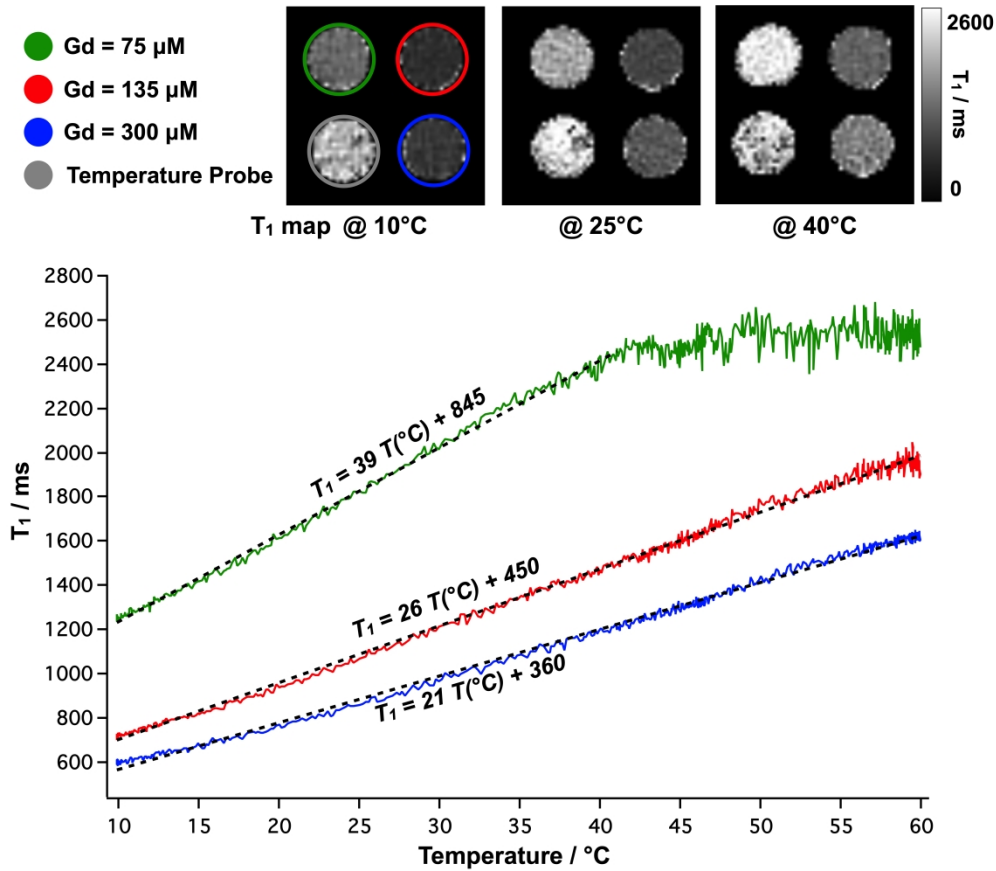
Chronogram of the 2D MS-MP2RAGE sequence. In this implementation, the usual MP2RAGE delays – namely T_1 , T_2 and $MP2RAGE_{TR}$ – are respectively set to 1000, 3000 and 9000 ms. GRE blocks of 640 ms were set. Other delays are shown on the chronogram of Slice 3. The interleaving of the six slices is shown.

521x285mm (300 x 300 DPI)



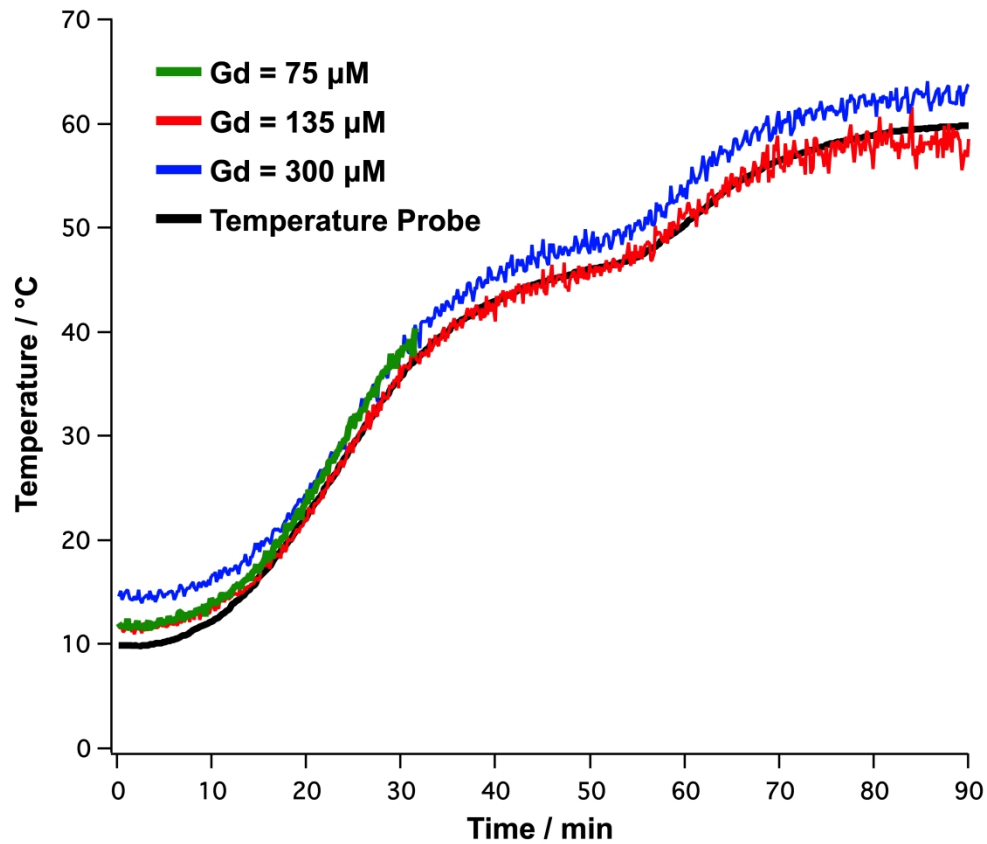
Impact of the inversion selectivity and inter-slice gap on the T₁ measurements. a) Relative T₁ difference (in percent) between MS-MP2RAGE and IR measurements using Gaussian (grey), Hermitian (hatch) or Cardinal sine (black) excitation pulses as a function of the inversion slab coverage (expressed in percentage of the 1-mm excitation slice thickness). b) T₁ measurements on six different slices located on the tube containing 75 μM Gd (T₁=1852 ms measured by IR, dashed line), as a function of the gap between each slice. The gap was increased from 0% to 25%, 50% and 100%. For each slice, the mean T₁ over the five experiments is represented by a dot. For each gap, the mean T₁ (cross) and the corresponding error bar over all six slices are shown. The 1-mm slices were acquired with an interlaced scheme, using an inversion slab set at 150% and a sinc3 excitation pulse.

588x222mm (300 x 300 DPI)



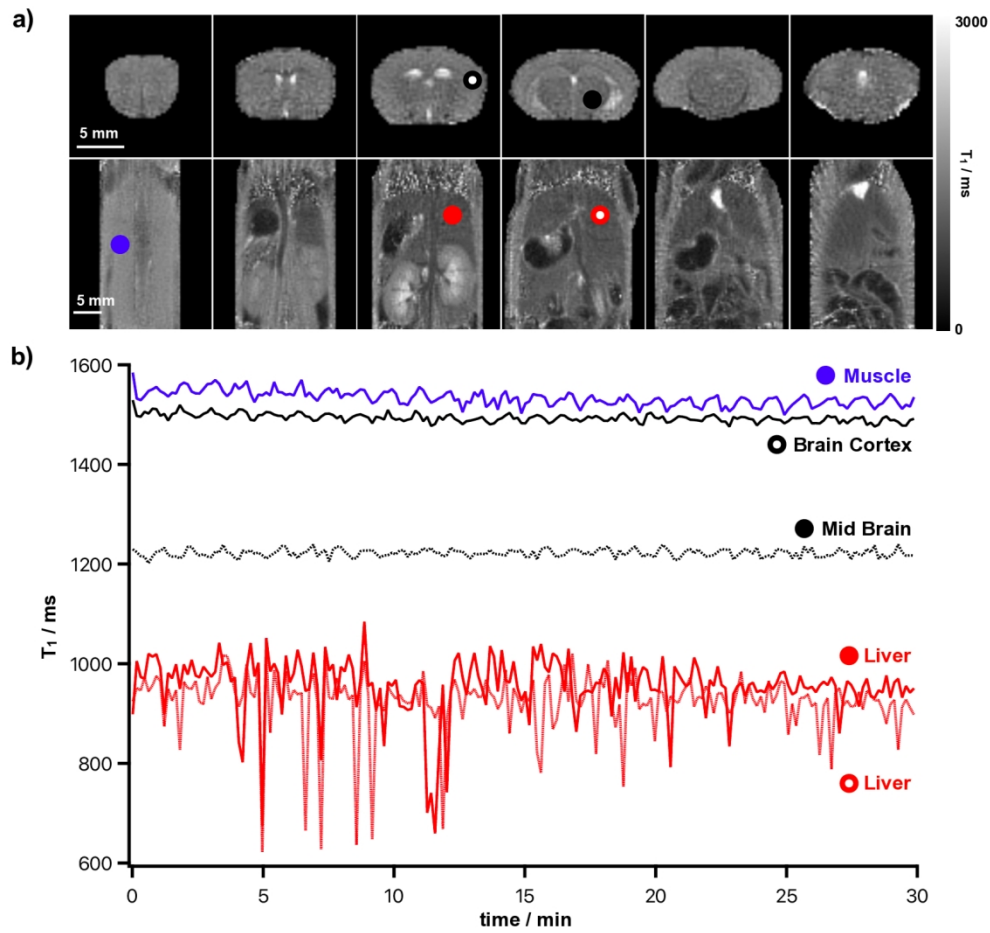
35 T₁ measurements while heating. a) Three representative axial T₁ maps (top) of agarose gels containing Gd
 36 at 75 (green), 135 (red) and 300 (blue) μM acquired at three temperatures (10°C, 25°C and 40°C). The
 37 tube encircled in gray contains the temperature probe. b) Graph showing the T₁ measured in the three
 38 corresponding Gd-containing tubes as a function of the temperature measured with the probe. For each
 39 tube, the linear equation of T₁ dependence on temperature is calculated using linear regression.

40 465x405mm (300 x 300 DPI)



Temperature monitoring. The mean slopes and intercept (A and T10) were calculated over three experiments, and used to estimate temperature warming during an independent experiment. The temperatures were estimated within the three Gd-containing tubes 75 (green), 135 (red) and 300 (blue) μM in the slice at the location of the probe (black solid line). The circulating water was first warmed to 60°C for 50 minutes, then to 80°C for 40 minutes, explaining the inflexion around 50 minutes.

330x279mm (300 x 300 DPI)



T1 evolution in vivo over 30 minutes. a) Six axial T1 maps of the brain (first row) and six coronal T1 maps of the abdomen (second row) were acquired with 1-mm slice thickness, spaced by 0.5 mm. Each six slices set was acquired in 9 s, while free breathing. b) T1 evolution in mouse back muscle (blue), in two slices containing the liver (red full and dashed lines), in the mouse midbrain (black dashed line) and brain cortex (black full line) are shown.

1463x1393mm (30 x 30 DPI)